State of Health Estimation of Lithium-Ion Batteries: A Multiscale Gaussian Process Regression Modeling Approach

Yi-Jun He, Jia-Ni Shen, and Ji-Fu Shen
Dept. of Chemical Engineering, Shanghai Electrochemical Energy Devices Research Center, Shanghai Jiao Tong University, Shanghai 200240, China

Zi-Feng Ma
Dept. of Chemical Engineering, Shanghai Electrochemical Energy Devices Research Center, Shanghai Jiao Tong University, Shanghai 200240, China

Sinopoly Battery Research Center, Shanghai 200241, China

DOI 10.1002/aic.14760
Published online March 2, 2015 in Wiley Online Library (wileyonlinelibrary.com)

Accurate state of health (SOH) estimation in lithium-ion batteries, which plays a significant role not only in state of charge (SOC) estimation but also in remaining useful life (RUL) prognostics is studied. SOC estimation and RUL prognostics often require one-step-ahead and long-term SOH prediction, respectively. A systematic multiscale Gaussian process regression (GPR) modeling method is proposed to tackle accurate SOH estimation problems. Wavelet analysis method is utilized to decouple global degradation, local regeneration and fluctuations in SOH time series. GPR with the inclusion of time index is utilized to fit the extracted global degradation trend, and GPR with the input of lag vector is designed to recursively predict local regeneration and fluctuations. The proposed method is validated through experimental data from lithium-ion batteries degradation test. Both one-step-ahead and multi-step-ahead SOH prediction performances are thoroughly evaluated. The satisfactory results illustrate that the proposed method outperform GPR models without trend extraction. It is thus indicated that the proposed multiscale GPR modeling method can not only be greatly helpful to both RUL prognostics and SOC estimation for lithium-ion batteries, but also provide a general promising approach to tackle complex time series prediction in health management systems. © 2015 American Institute of Chemical Engineers *AIChE J*, 61: 1589–1600, 2015

Keywords: lithium-ion batteries, state of health, state of charge, remaining useful life, wavelet analysis, Gaussian process regression

Introduction

Lithium-ion batteries, as lightweight and high energy density power sources, are commonly used in portable electronic devices, electric and hybrid vehicles, etc. It has been widely recognized that accurate estimation of state of charge (SOC) and state of health (SOH) play significant roles in reliable and safe usage of lithium-ion batteries.[1] However, traditional battery management system has mostly focused on addressing the SOC issue with limited attention to SOH.[2,3] In general, the loss of capacity in lithium-ion batteries results from a complex combination of two or more of the following factors: loss of active material, decomposition of electrolyte, formation of films on the anode and/or the cathode, degradation and increased impedance of the electrodes, dissolution of the current collector, and so forth.[4] Various electrochemical models have been developed to understand the complex mechanism of the degradation processes occurring in the lithium-ion batteries.[4–6] However, first-principle models often need high computing complexity and have not been ready for meeting the real-time prognostics requirement of SOH. Moreover, the values of parameters in first-principle models may differ from one battery to another, or from one cycle to the next for the same battery,[7] which further complicates the first-principle model-based SOH estimation and calls for accurate and rapid online parameter estimation techniques.

Recently, both electrochemical models and data-driven models-based SOH prognostics techniques have been developed. Extended kalman filter (EKF) has been applied to state estimation of equivalent circuit model for SOH prediction of batteries.[8,9] However, EKF would accumulate significant prediction errors for long-term prediction and lacks uncertainty management in SOH prognostics. Sequential Monte Carlo methods, also referred to as particle filtering (PF) methods, have attracted significant attentions to SOH and remaining useful life (RUL) predictions.[2,3,10–14] PF is capable of combining information available from system measurements and analytic/empirical models and is proved to be useful for

Correspondence concerning this article should be addressed to Z.-F. Ma at zfma@sjtu.edu.cn.

representing uncertainty in the prognostics of degradation processes by providing a probability density function for SOH and RUL of batteries.[2,3] The most data-driven techniques such as neural networks,[15] fuzzy logic,[16] regressions,[17] distributed active learning,[18] and relevance vector machine[19] lack specific strategies in dealing with model uncertainties and would lead to prognostics performance deterioration in case facing long-term changes in environmental and operating conditions. Gaussian process regression (GPR)[20] could provide a confidence measure of output and has been used to SOH and RUL predictions.[11,21] Note that data-driven techniques avoid developing complex physical models and often have lower computational cost for meeting the real-time prognostics requirements. However, data-driven techniques often need sufficient training data for properly learning the nonlinear dynamics of processes.

It has been recognized that the existence of regeneration phenomena[2,3,13,21] in lithium-ion batteries has significant effect on the accuracy and precision of SOH prognostics. A particle-filtering-based prognostics framework has been developed by detecting and isolating the effect of regeneration phenomena within the life-cycle model.[3] An improved GPR method, namely combination Gaussian process functional regression, has been proposed to capture regeneration phenomena.[21] Because the rate of capacity fade is highly dependent on operating conditions such as ambient temperature, charge/discharge current rate, and aging periods, a historical time series of SOH contains abundant process operational information of lithium-ion batteries. Additionally, inherent differences in manufacturing assemblies and material properties would lead to the variations in the degradation process of batteries. Hence, the parameters in electrochemical model-based prognostics method are suffering from uncertainties and need to be online reconciliation, which would consequently increase the difficulty of accurate SOH estimation. Data-driven techniques, which directly utilize historical SOH time series to construct prediction models, would provide an alternative solution of SOH estimation with low computational cost. However, recent studies directly use raw SOH time series to establish the prediction model, and consequently it would fail to extract correct global degradation trend from raw SOH time series buried with complex local regeneration and fluctuations. Moreover, as traditional analyses of time series typically require that the data under study to be stationary, long-term prediction of raw SOH time series with nonlinear, nonstationary, and multiscale characteristics is still a challenging task.

Note that a SOH time series is reasonable to be considered as a hybrid signal with multiscale components, where global degradation, local regeneration, and fluctuations are supposed to be of different scales. It is, therefore, important to decouple those correlative components from original SOH time series for extracting the most useful information. Otherwise, prediction model, directly established based on the raw SOH time series, not only probably has little physical sense, but also probably has poor generalization performance. As the actual usable capacity of lithium-ion batteries should be accurately predicted at the beginning of each charge/discharge cycle and plays an important effect on SOC estimation, it requires performing rapid and accurate one-step-ahead SOH prediction. While for the RUL prognostics, long-term SOH prediction should be performed. We realize that correct extraction and modeling of global degradation trend is the most important task for long-term SOH estimation while local regeneration and fluctuations should be accurately captured in one-step-ahead SOH prediction. Moreover, it is recognized that recent studies lack a systematic performance evaluation of SOH estimation method for both one-step-ahead and long-term prediction in a unified framework. Hence, this study focuses on proposing a unified multiscale GPR modeling approach to satisfy the accuracy and computational speed requirements for both one-step-ahead capacity prediction in SOC estimation and long-term SOH prediction in RUL prognostics. We first utilize wavelet decomposition method[22] to decouple global degradation trend, local regeneration trend, and fluctuations in SOH time series. Then GPR model with time index is adopted to fit the global degradation trend, and GPR models with lag vector are used to predict local regeneration and fluctuations at different scales. Finally, these GPR models at different scales are integrated to achieve SOH prediction.

The reminder of this article is structured as follows. The problem of multi-step-ahead SOH prediction is first stated. Then, we propose a systematic wavelet analysis-based multiscale GPR modeling method. The proposed model is then applied to SOH estimation of lithium-ion batteries. Finally, conclusions are provided.

Methodology

Problem statement of multi-step-ahead prediction of SOH

Given a historical time series of SOH represented by $S_{1:T}=\{s(1),s(2),\cdots,s(T)\}$, the prognostics problem for SOH is to estimate with M-step ahead

$$\hat{S}_{T+1:T+M}=\{\hat{s}(T+1),\hat{s}(T+2),\cdots,\hat{s}(T+M)\} \tag{1}$$

An optimal predictor for $\hat{s}(T+j)$ is given by

$$\hat{s}_{T+j}=\mathrm{E}[s(T+j)|s(T),s(T-1),\cdots,s(1)] \tag{2}$$

where $\mathrm{E}[\cdot]$ denotes the expectation.

Note that one-step-ahead SOH prediction is a special case of multi-step-ahead prediction with $M=1$. In contrast to one-step-ahead prediction, multi-step-ahead prediction ($M>1$) often suffers accumulation of errors and increasing uncertainties, which makes long-term time series prediction inherently more difficult. Traditional strategies for long-term time series prediction can be broadly divided into two classes: direct method and recursive method. The direct method for multi-step-ahead prediction involves establishing a set of M prediction models and often requires a higher computational cost. For the recursive method, one-step-ahead prediction is repeated up to the desired step, where the future series value estimated from one-step-ahead prediction model is recursively fed back as an input to the following prediction. Although the recursive method shows lower computational cost, it usually suffers propagation of prediction uncertainty, which will gradually accumulate prediction errors as the prediction step progresses. Recently, novel strategies, such as combination method of direct and recursive (DirRec), multi-input multi-output (MIMO) strategy, and combination method of direct and MIMO (DIRMO), have been developed to perform long-term prediction. However,

there is no definite indication of superiority of one strategy over the others.[23,24]

It has been widely recognized that prediction of nonlinear and nonstationary time series with increase/decrease trend often requires an important preprocessing step of detrending.[25] In this study, it is realized that the trend in SOH time series itself is important and needs to be modeled for estimating the capacity degradation. However, extracting the real trend from SOH time series is often a challenging task. As the trend is corrupted by fluctuations, direct modeling of raw SOH time series may determine an incorrect trend and consequently deteriorate the prediction performance. It is, therefore, necessary to decouple the trend and fluctuations before constructing the prediction model. Besides lack of trend extraction for SOH estimation, recent studies often adopt a specified function forms[12,14,19] such as the sum of two exponential functions to model the capacity degradation data, which might be lack of flexibility for various lithium-ion batteries with different capacity degradation mechanisms and fail to correctly fit the capacity degradation data when local optimization method is adopted. Hence, in this study, after decoupling of raw SOH time series based on wavelet analysis method, GPR, as a universal function approximator, is applied to quantitate modeling of global degradation trend and fluctuations at different scales.

Wavelet analysis method

Wavelet analysis is a powerful time-frequency tool for analysis of nonstationary and transitory signals and has been widely applied in various fields,[22] such as signal processing, image processing, data compression, and financial time series. In wavelet analysis, at high frequencies (corresponding to small scales), narrow windows are used to get precise time resolution, whereas at low frequencies (corresponding to large scales), wide windows are used to get finer frequency resolution. Wavelet analysis is, therefore, often regarded as a mathematical "microscope" that is able to examine different parts of the signal by automatically adjusting the focus. In this study, it is assumed that the global degradation trend in SOH time series is of low frequency and the local regeneration trend and fluctuations are of high frequency.

Wavelet analysis utilizes the wavelet function $\varphi(t)$ and scaling function $\phi(t)$ to perform the multirelsolution analysis (MRA) decomposition and reconstruction of the signal. The wavelet function serving as a high-pass filter can generate the detailed version of the given signal, while the scaling function serving as a low-pass filter can generate the approximated version of the given signal. The recursive mathematical representation of MRA can be defined as follows

$$V_{j-1}=W_j\oplus V_j=W_j\oplus W_{j+1}\oplus\cdots\oplus W_{j+E}\oplus V_{j+E} \tag{3}$$

where V_j and W_j are the approximated and detailed versions of the given signal on level j, respectively, $\oplus$ denotes a orthogonal summation of two decomposed signals, and E is the number of decomposition levels.

The discrete wavelet transform (DWT) is an MRA technique, where the original signal can be decomposed into several signals with different scales and can reconstruct the signals using inverse DWT. In DWT, a discrete time series can be expanded as a sum of sets of base functions $\varphi_{j,k}(t)$ and $\phi_{j,k}(t)$ produced by dilations and translations of the orthogonal wavelet function $\varphi(t)$ and scaling function $\phi(t)$. The details of DWT can be referred to Misiti's et al. book.[22] Note that the type of wavelet function and the number of decomposition level will affect the performance of prediction model. The principle for determine the decomposition level in this study is to ensure that the extracted approximated signal is monotonic. In this study, Daubechies fourth-order wavelet is utilized and the decomposition level of is set equal to 5. In addition, the decomposed approximated signal of original SOH time series is treated as global degradation trend and the detailed signals at different scales correspond to local regeneration trend and fluctuations in SOH time series.

GPR model

Gaussian process model is a flexible nonparametric model in the Bayesian framework, which could provide not only the mean value but also the variance of the conditionally expected value of the output. GPR models have been widely applied to multi-step-ahead predictions in time series analysis.[26–29] The Gaussian process is defined as a collection of a finite number of random variables with joint multivariable Gaussian distribution

$$f(\boldsymbol{x}_1),f(\boldsymbol{x}_2),\cdots,f(\boldsymbol{x}_N)\sim\mathcal{N}(\boldsymbol{m}(\boldsymbol{X}),\boldsymbol{\Sigma}) \tag{4}$$

where $\boldsymbol{X}=[\boldsymbol{x}_1,\boldsymbol{x}_2,\cdots,\boldsymbol{x}_N]$, $\boldsymbol{m}(\boldsymbol{X})$ is the mean function, $\boldsymbol{\Sigma}$ is the covariance matrix, and $f(\cdot)$ is a function that generates data points. Note that selection of the proper forms of mean and covariance functions could take a positive effect on the prediction performance. The SOH time series shows a nonstationary characteristics, a linear mean function is utilized to capture the decrease trend, which is represented by a linear combination of the input shown as

$$\boldsymbol{m}(\boldsymbol{X})=\tilde{\boldsymbol{X}}\boldsymbol{\theta}_h \tag{5}$$

where $\tilde{\boldsymbol{X}}=[\boldsymbol{X}\vdots\boldsymbol{e}]$ is an augment input matrix and $\boldsymbol{\theta}_h=[\theta_{h0},\theta_{h1},\cdots,\theta_{hH}]^{\mathrm{T}}$ is unknown hyperparameters in mean function.

The covariance $\Sigma_{pq}=\mathrm{Cov}\left(f\left(\boldsymbol{x}_p\right),f\left(\boldsymbol{x}_q\right)\right)=k\left(\boldsymbol{x}_p,\boldsymbol{x}_q\right)$ gives the covariance between the points $f\left(\boldsymbol{x}_p\right)$ and $f\left(\boldsymbol{x}_q\right)$ and is a function of the inputs $\boldsymbol{x}_p$ and $\boldsymbol{x}_q$. Two common types of covariance functions, that is, squared exponential and periodic covariance functions, are shown as

$$k_{\mathrm{SE}}\left(\boldsymbol{x}_p,\boldsymbol{x}_q\right)=\sigma_{\mathrm{SE}}^2\exp\left[-\|\boldsymbol{x}_p-\boldsymbol{x}_q\|^2/2\ell_{\mathrm{SE}}^2\right] \tag{6}$$

$$k_{\mathrm{P}}\left(\boldsymbol{x}_p,\boldsymbol{x}_q\right)=\sigma_{\mathrm{P}}^2\exp\left[-2\sin^2\left(\frac{\omega}{2\pi}\|\boldsymbol{x}_p-\boldsymbol{x}_q\|\right)/\ell_{\mathrm{P}}^2\right] \tag{7}$$

where σ_{SE}^2 and σ_{P}^2 are the variances, ℓ_{SE} and ℓ_{P} are the characteristic length-scales, ω is the angular frequency, and $\|\cdot\|$ denotes the Euclidean norm. The overall variance of the random function can be controlled by the above hyperparameters. Proper selection of covariance function is problem-specific, and combination of different covariance function is often utilized. In this study, it is found that a squared exponential or periodic covariance function with a linear mean function is sufficient to fit the degradation trend after removing the local regeneration and fluctuations.

For performing SOH regression, we assume the availability of a set of N training points $\{(\boldsymbol{x_i},\boldsymbol{y_i})|i=1,\cdots,N\}$ and the tragets $\boldsymbol{y}$ is described as

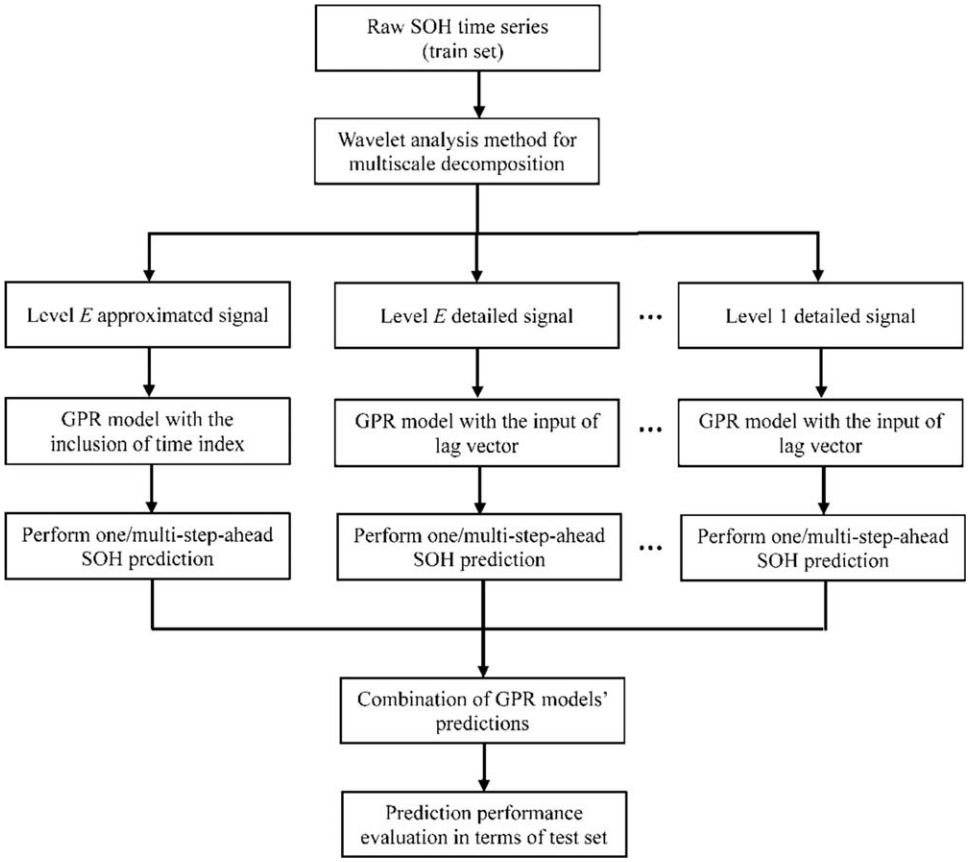

Figure 1. Schematic of wavelet analysis-based GPR modeling method.

$$\boldsymbol{y}=f(\boldsymbol{x})+\varepsilon \tag{8}$$

where ε is the additive noise following an independent, identically distributed Gaussian distribution with zero mean and variance σ_n^2, namely $\varepsilon \sim \mathcal{N}(0,\sigma_n^2)$.

The accuracy of SOH prediction depends on the unknown hyperparameters in both mean and covariance functions $\boldsymbol{\Theta}=[\boldsymbol{\theta},\boldsymbol{\sigma},\ell,\boldsymbol{\omega}]^{\mathrm{T}}$ and, therefore, these hyperparameters needs to be optimized. The training of GPR model is carried out by minimizing the negative marginal log-likelihood function given by

$$J=-\log\ p(\boldsymbol{y}|\boldsymbol{X},\boldsymbol{\Theta})=\frac{1}{2}\log|\boldsymbol{K}|+\frac{1}{2}(\boldsymbol{y}-\boldsymbol{m}(\boldsymbol{X}))^{\mathbf{T}}\boldsymbol{K}^{-1}(\boldsymbol{y}-\boldsymbol{m}(\boldsymbol{X}))+\frac{N}{2}\log\ 2\pi \tag{9}$$

where $\boldsymbol{K}=\boldsymbol{\Sigma}+\sigma_n^2\boldsymbol{I}$ is the covariance matrix for the noisy targets $\boldsymbol{y}$ and $\boldsymbol{I}$ is the identity matrix of same dimensions as $\boldsymbol{K}$. $\frac{1}{2}\log|\boldsymbol{K}|$ is the complexity penalty depending on the covariance function and the inputs. Note that the model complexity decreases with the increasing of length-scale. A conjugate gradient method is utilized to optimize the hyperparameters in this study.

For a new test input $\boldsymbol{x}_*$, the prior distribution for GPR is described as follows

$$\begin{bmatrix}\boldsymbol{y}\\ y_*\end{bmatrix}\ \sim\ \mathcal{N}\left(\begin{bmatrix}\boldsymbol{m}(\boldsymbol{X})\\ \boldsymbol{m}(\boldsymbol{x}_*)\end{bmatrix},\begin{bmatrix}\boldsymbol{K} & \boldsymbol{k}(\boldsymbol{x}_*,\boldsymbol{X})\\ \boldsymbol{k}^{\mathrm{T}}(\boldsymbol{x}_*,\boldsymbol{X}) & k(\boldsymbol{x}_*,\boldsymbol{x}_*)\end{bmatrix}\right) \tag{10}$$

where $\boldsymbol{k}(\boldsymbol{x}_*,\boldsymbol{X})=[k(\boldsymbol{x}_*,\boldsymbol{x}_1),k(\boldsymbol{x}_*,\boldsymbol{x}_2),\cdots,k(\boldsymbol{x}_*,\boldsymbol{x}_N)]^{\mathrm{T}}$.

The posterior distribution for the above test input is

$$p(y_*|\boldsymbol{X},\boldsymbol{y},\boldsymbol{x}_*)\ \sim\ \mathcal{N}\left(\hat{y}_*,\sigma_{\hat{y}_*}^2\right) \tag{11}$$

where $\hat{y}_*$ and $\sigma_{\hat{y}_*}^2$ are the predictive mean and variance, respectively, and are calculated by

$$\hat{y}_*=\boldsymbol{m}(\boldsymbol{x}_*)+\boldsymbol{k}^{\mathrm{T}}(\boldsymbol{x}_*,\boldsymbol{X})\boldsymbol{K}^{-1}(\boldsymbol{y}-\boldsymbol{m}(\boldsymbol{X})) \tag{12}$$

$$\sigma_{\hat{y}_*}^2=k(\boldsymbol{x}_*,\boldsymbol{x}_*)-\boldsymbol{k}^{\mathrm{T}}(\boldsymbol{x}_*,\boldsymbol{X})\boldsymbol{K}^{-1}\boldsymbol{k}(\boldsymbol{x}_*,\boldsymbol{X})+\sigma_n^2 \tag{13}$$

In this study, for fitting the global degradation trend, the input $\boldsymbol{x}$ is set as time index and a linear mean function is adopted; while for modeling the local regeneration and fluctuations at different scales, the input $\boldsymbol{x}$ is set as lag vector and a constant mean function is adopted.

Wavelet analysis-based GPR modeling method

As shown in Figure 1, the modeling steps of wavelet analysis-based GPR modeling method is briefly described as follows:

1. Apply DWT to decompose the original SOH time series into E detailed signals at different scales and one approximated signal, where E is the number of decomposition levels.

2. Independently construct SOH prediction models for approximated and detailed signals by GPR method. For the approximated signal, the input of GPR model is time index, and a linear mean function and squared exponential covariance function are used; while for the detailed signals, the input of GPR model is lag vector, a constant mean function is used, and both squared exponential and periodic covariance functions are compared.

3. Obtain the final prediction results by aggregating the prediction results of all GPR models, and calculate the performance criteria, namely the mean absolute percentage error (MAPE) and root mean square error (RMSE).

MAPE and RMSE are defined as Eqs. 14 and 15, respectively

$$\mathrm{MAPE}(\%)=\frac{100}{N}\sum_{i=1}^{N}\left|\frac{y_i-\hat{y}_*}{y_i}\right| \tag{14}$$

$$\mathrm{RMSE}=\sqrt{\frac{\sum_{i=1}^{N}(y_i-\hat{y}_*)^2}{N}} \tag{15}$$

The time complexity for training one GPR model is $O(N^3)$ by Eq. 9 as it involves inversion of the matrix, where N is the number of training samples. For training the multiscale GPR model, the time complexity becomes $O(E{\cdot}N^3)$. As the decomposition level E is significantly less than N, the time complexity of multiscale GPR model construction is $O(N^3)$. The time complexity involved in mean and variance prediction given by Eqs. 12 and 13 are $O(N)$ and $O(N^2)$, respectively, assuming that the inverse matrix has been stored from the training phase. For the recursive strategy-based long-term prediction, the inverse matrix does not change during recursive one-step-ahead prediction and the time complexity involved in prediction is $O(N^2)$

Both the decomposition level E and the length of lag vector would take effect on the prediction performance. In this study, the decomposition level and the length of lag vector are simply set equal to 5 and 1, respectively. In addition, optimal selection of initial values of hyperparameters in GPR models, which would also affect the prediction performance, is out of our scope, and we will simply set the initial values of hyperparameters as: for the global degradation trend GPR model, constant term of 1 and slope term of 0.5 in linear mean function, characteristic length-scale of 1 and variance of 1 in squared exponential covariance function; for GPR model of detailed signals, constant term of 1 in constant mean function, characteristic length-scale of 1, and variance of 1 in squared exponential covariance function, and characteristic length-scale of 1, variance of 1 and angular frequency of 1 in periodic covariance function.

Conversely, it has been found that adoption of combination of covariance functions could be greatly helpful for improving the prediction performance, because covariance functions with different scales can fit to different pattern exhibited in the data. GPR model with spectral mixture kernels[30] has been used to performance comparison in this study. For clarification, the proposed multiscale GPR methods with squared exponential and periodic covariance functions are called SE-MGPR and P-MGPR, respectively, and the GPR method with spectral mixture kernels is called SMK-GPR. For the SMK-GPR model, time index is used as the input and a linear mean function is adopted. The number of kernels is selected to be 3, the initial weights for each kernel are set equal to 1/3, and the initial values of other hyperparameters are simply set equal to 1. A MATLAB toolbox of GPML version 3.5 (http://www.gaussianprocess.org/gpml/code/matlab/doc/) is adopted to construct the GPR model and all computations are carried out on a PC with 2.60 GHz processor and 8 GB of RAM.

Results and Discussion

Raw data description of lithium-ion batteries

The aging data of lithium-ion batteries obtained from the data repository of the NASA Ames Prognostics Center of Excellence (PCoE) is used to illustrate the effectiveness of multiscale GPR method.[31] A set of commercial 18,650 lithium-ion batteries were run through three different operational profiles, namely charge, discharge, and impedance, at room temperature. Charging was carried out in a constant current mode at 1.5 A until the battery voltage reached 4.2 V and then continued in a constant voltage mode until the charge current dropped to 20 mA. Discharge was carried out at a constant current level of 2 A until the battery voltage fell to 2.7, 2.5, and 2.2 V for batteries No. 5, 6, and 7, respectively. Impedance measurement was conducted by an electrochemical impedance spectroscopy (EIS) frequency from 0.1 Hz to 5 kHz. Repeated charge and discharge cycles resulted in accelerated aging of the batteries while impedance measurements provide insight into the internal battery parameters that change as aging progresses. The experiments were stopped when the batteries reached end-of-life criteria, which was a 30% fade in rated capacity (from 2 to 1.4 Ah). This dataset can be used for the prediction of both SOC and SOH. SOH is typically defined as the ratio of the current capacity over the nominal capacity of a fresh battery, which can be easily derived from the experimental capacity data.

Figure 2 shows the evolution of SOH for batteries No. 5, 6, and 7. The total charge/discharge cycles are all 168 for these three batteries. It can be seen from Figure 2 that the SOH time series shows a clear regeneration phenomenon and local fluctuations, and the global degradation trend also shows a multiscale characteristics, where capacity exists different degradation rates at different cycles. It is, therefore, important to perform multiscale decomposition of SOH time series for further prediction model construction. Note that in practical industrial applications, the number of degradation data samples would be much larger than this dataset of 168. Moreover, with the development of lithium-ion batteries technology, the life of commercial lithium-ion batteries have exceeded 1000 charge/discharge cycles, which could alleviate the small sample problem in SOH prediction.

Apart from the capacity-based SOH indication, the internal resistance has been used as another indication for characterizing SOH. Note that the capacity and internal resistance characterize the useful energy and attainable power to some extent respectively. Hence, both SOH indications should be simultaneously used in RUL prognostics for systematical evaluation of energy and power degradation. The internal resistance can be broadly classified into ohmic resistance and polarization resistance. It has been recognized that the internal resistance not only depends on degradation, but also depends on operating conditions such as temperature and SOC. Furthermore, it has been found that the internal resistance is much more sensitive to the temperature changes than to degradation. Hence, the internal resistance-based SOH indication should exclude the other factors except degradation. Figure 3 shows the estimated internal resistance from EIS data for batteries No. 5, 6, and 7, where the internal resistance is calculated through the sum of ohmic and polarization resistances. It can be observed from Figures 2 and 3 that battery No. 6 with high degradation rate has a higher internal resistance than batteries No. 5 and 7. Although the capacity and internal resistance show decreasing and

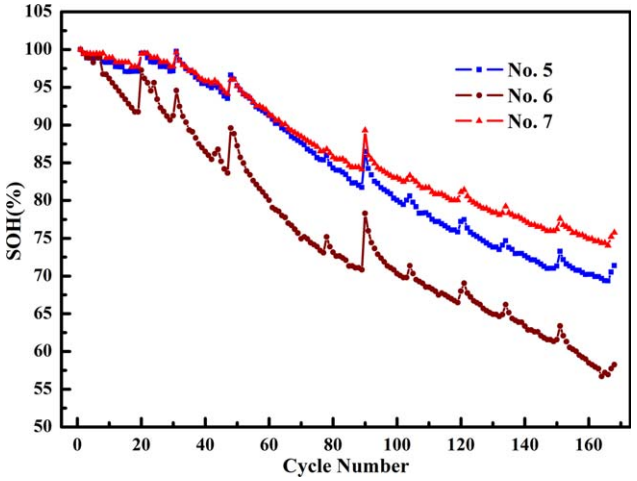

Figure 2. Evolution of SOH for three lithium-ion batteries.

[Color figure can be viewed in the online issue, which is available at wileyonlinelibrary.com.]

increasing trends, respectively, the capacity regeneration does not coincide with an exact internal resistance growth for three batteries. It is, therefore, indicated that although aging related changes in capacity and internal resistance usually point in almost the same degradation direction, both SOH indications are not directly coupled. This study only focuses on adoption of capacity degradation for quantification of SOH.

Multiscale characteristics of SOH time series

Figures 4–6 show the wavelet decomposition of SOH time series for batteries No. 5–7, respectively. The extracted approximated signals are shown in Figures 4A, 5A, and 6A, and the detailed signals are shown in Figures 4B–F, 5B–F, and 6B–F. It can be easy to see that the extracted approximated signals show monotonic decrease trend and both high-frequency peaks and low-frequency fluctuations are removed. In addition, compared to the original SOH time series, the approximated signals can capture the global degradation trend with a small discrepancy. It is expected that long-term

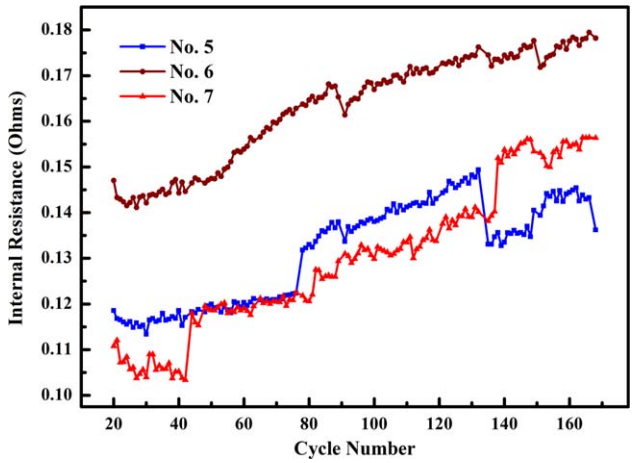

Figure 3. Evolution of internal resistance for three lithium-ion batteries.

[Color figure can be viewed in the online issue, which is available at wileyonlinelibrary.com.]

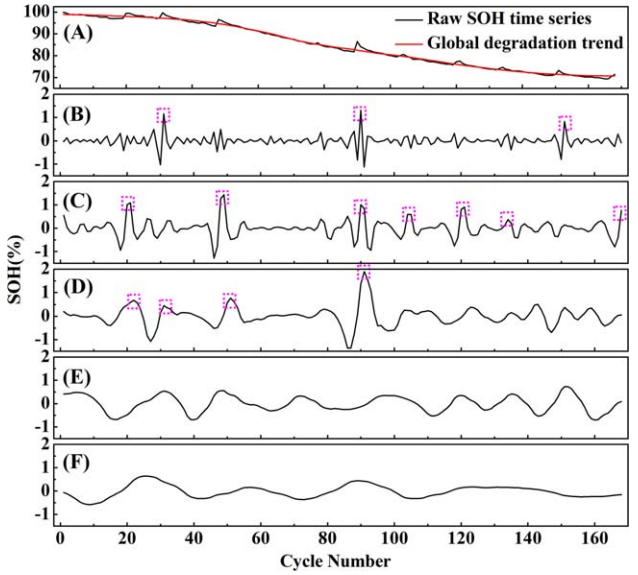

Figure 4. Wavelet decomposition of SOH time series for battery No. 5: (A) approximated signal; (B) level 1; (C) level 2; (D) level 3; (E) level 4; (F) level 5.

[Color figure can be viewed in the online issue, which is available at wileyonlinelibrary.com.]

SOH prediction model based on the approximated signals would be able to track the correct degradation trend by removing fluctuations, which has been validated by the results of long-term SOH prediction. It is also observed that the peaks corresponding to capacity regeneration can be almost captured by level 1–3 detailed signals. Based on the amplitude and location of peaks labeled with dashed square, it is found that the variations of strength of local capacity regeneration at different charge/discharge cycles would take

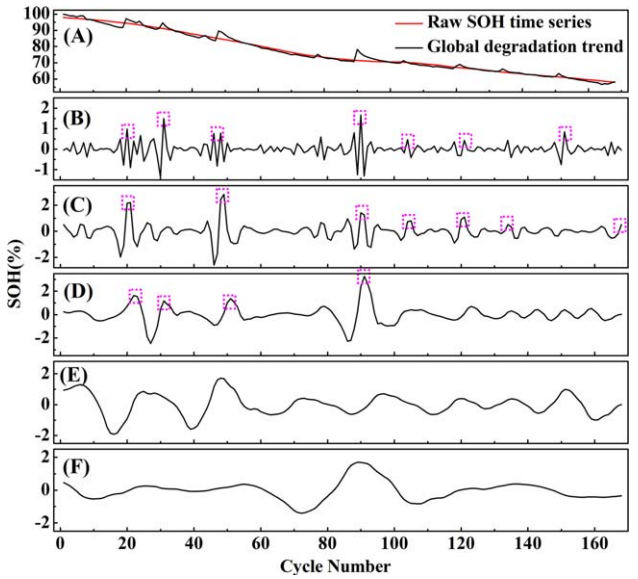

Figure 5. Wavelet decomposition of SOH time series for battery No. 6: (A) approximated signal; (B) level 1; (C) level 2; (D) level 3; (E) level 4; (F) level 5.

[Color figure can be viewed in the online issue, which is available at wileyonlinelibrary.com.]

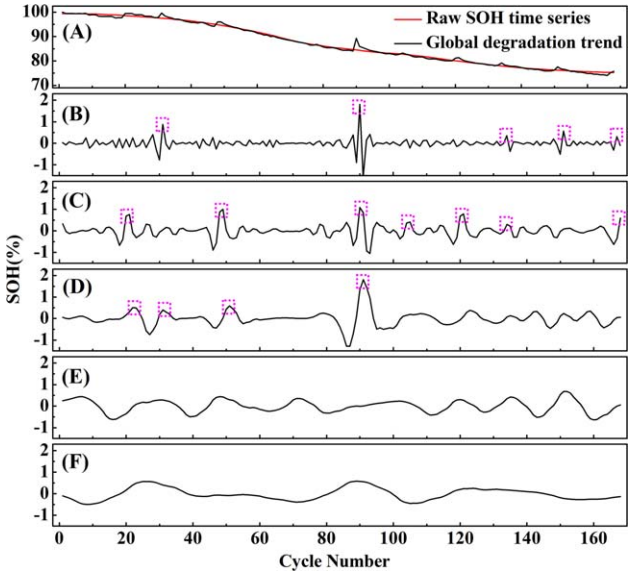

Figure 6. Wavelet decomposition of SOH time series for battery No. 7: (A) approximated signal; (B) level 1; (C) level 2; (D) level 3; (E) level 4; (F) level 5.

[Color figure can be viewed in the online issue, which is available at wileyonlinelibrary.com.]

effects on the amplitude distribution at different scales. Meanwhile, the peaks corresponding to high and low capacity regeneration are mainly captured by level 2–3 detailed signals and level 1–2 detailed signals, respectively. The level 4–5 detailed signals are considered to be low-frequency performance fluctuations in lithium-ion batteries. It should be noted that such a partition between local regeneration and fluctuations are scratchy and local fluctuations often coexist with regeneration at level 1–3 detailed signals. However, it is reasonable to conclude that the SOH time series exhibit obvious multiscale characteristics.

Figure 7 shows the energy percentage among level 1–5 detailed signals for three batteries. It is found that three batteries show different energy distributions of the level 1–5 detailed signals, which might be an indication for comparing the performance of different batteries. It is also seen that the level-3 detailed signal has the maximum energy percentage

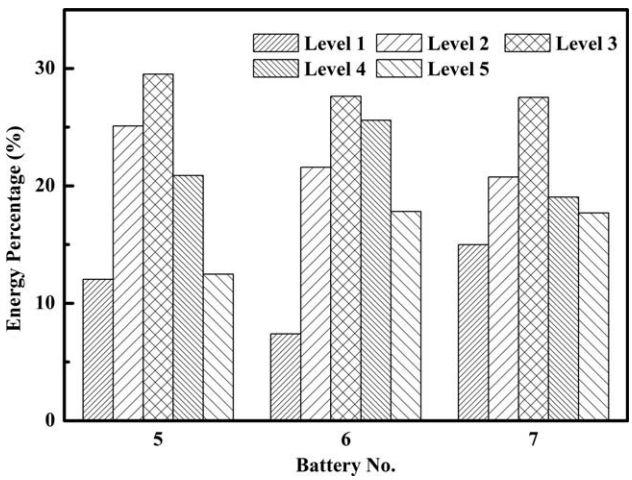

Figure 7. Energy percentage of detailed signals at different levels for three lithium-ion batteries.

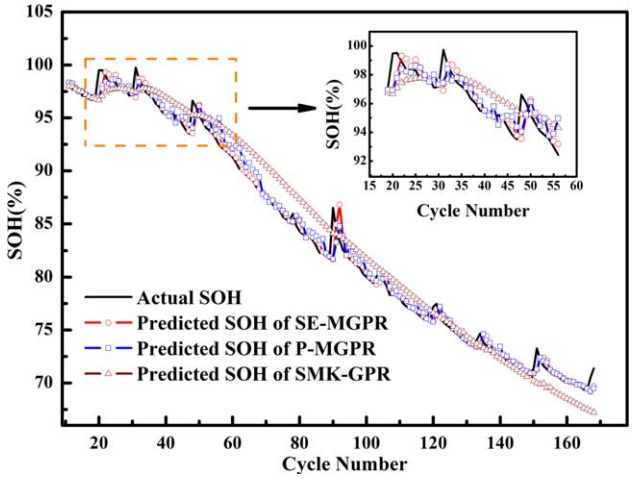

Figure 8. One-step-ahead SOH prediction for battery No. 5.

[Color figure can be viewed in the online issue, which is available at wileyonlinelibrary.com.]

for these three batteries. The values of absolute energy in level-3 detailed signals are 29, 89, and 21 for batteries No. 5, 6, and 7, respectively. From Figure 2, it is observed that battery No. 6 has high regeneration capacity, while batteries No. 5 and 7 have relatively low regeneration capacities. Hence, the level-3 detail signal might be served as an appropriate indication for high regeneration capacity. In addition, it is found that the energy percentage of level-1 detailed signal might be an indication of the capacity degradation rate of batteries, where battery No. 6 with high capacity degradation rate has minimum energy percentage of level-1 detailed signal and battery No. 5 with low capacity degradation rate has maximum energy percentage of level-1 detailed signal. However, it should be noted that these indications obtained from energy distribution of detailed signals should be further verified by investigating much more batteries life testing. It is expected that through combining with bottom-up capacity degradation mechanism analysis and experimental characterization, more useful information could be extracted from top-down multiscale analysis of SOH time series, which would

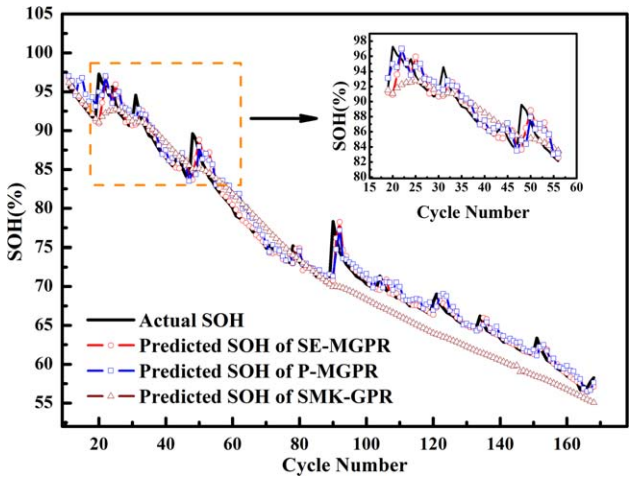

Figure 9. One-step-ahead SOH prediction for battery No. 6.

[Color figure can be viewed in the online issue, which is available at wileyonlinelibrary.com.]

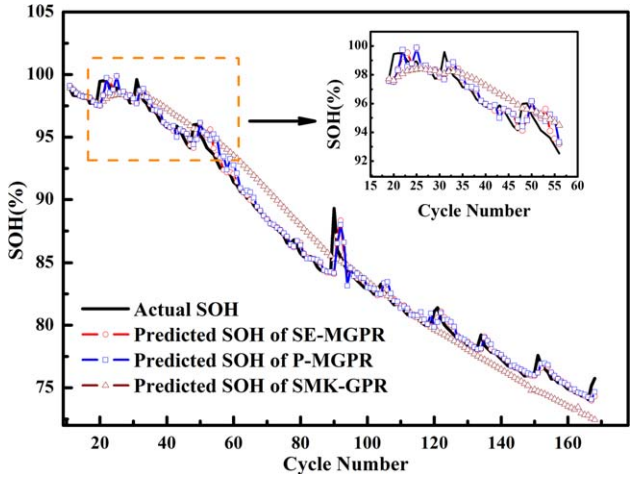

Figure 10. One-step-ahead SOH prediction for battery No. 7.

[Color figure can be viewed in the online issue, which is available at wileyonlinelibrary.com.]

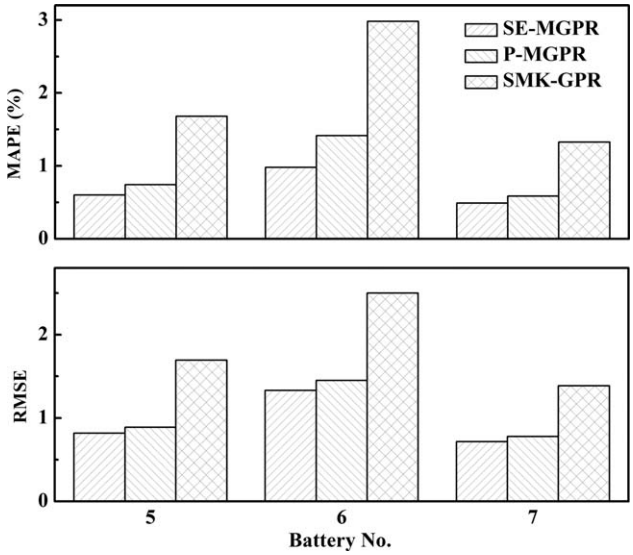

Figure 12. MAPE and RMSE of one-step-ahead SOH prediction for three batteries.

be great helpful for the construction of accurate SOH prediction model.

One-step-ahead SOH prediction

Accurate and rapid implementation of one-step-ahead SOH prediction is important to SOC estimation. Figures 8–10 show the one-step-ahead SOH prediction using SE-MGPR, P-MGPR, and SMK-GPR for batteries No. 5–7, respectively. The one-step-ahead prediction horizon is from cycle 11 to cycle 168. The data point is recursively added into the training set and the GPR model is updated step-by-step. For example, to predict for cycle 100, data from previous 99 cycles was used. From Figure 8, it is observed that the predicted values of both SE-MGPR and P-MGPR almost coincide with the actual SOH values, but the predicted values of SMK-GPR show relatively large deviations from the actual SOH values. The one-step-ahead prediction from Figures 9 and 10 also show the similar results as Figure 8. It is implied that the multiscale GPR modeling approach could provide very satisfactory prediction performance and follow the fluctuations. Although SMK-GPR method theoretically serves an outstanding approach to discover patterns with different scales, the optimization of a relatively larger number of hyperparameters in SMK-GPR becomes more difficult and is easily trapped into local optimum. Furthermore, the intrinsic nonstationary and multiscale characteristics in SOH time series might also attribute to a relatively large prediction discrepancy of SMK-GPR. It is, therefore, validated that the multiscale decomposition of SOH time series can be greatly helpful to improve the prediction performance.

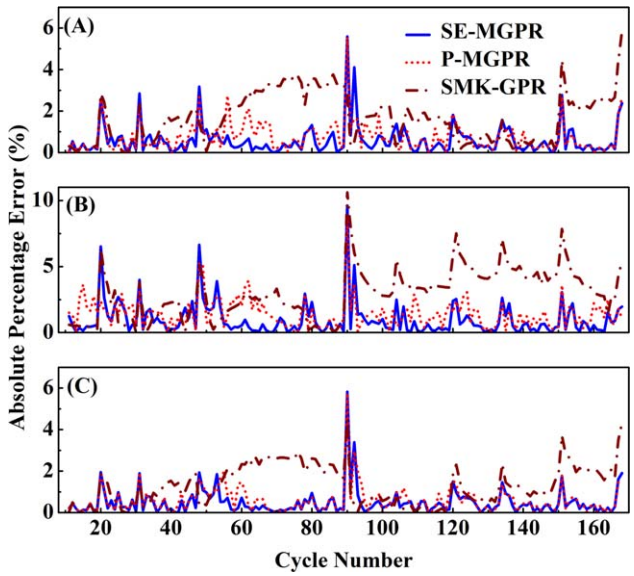

Figure 11. APE of one-step-ahead SOH predication for three batteries: (A) No. 5; (B) No. 6; (C) No. 7.

[Color figure can be viewed in the online issue, which is available at wileyonlinelibrary.com.]

It is found from the enlarged view in Figures 8–10 that if a local regeneration is occurred, both SE-MGPR and P-MGPR cannot timely response and there almost exists one time step delay. The one-time step delay might be attributed to the fact that the structure of covariance function ensures that locations close to each other in the feature space have similar output values. When a regeneration peak is observed in data, although the multiscale GPR model cannot capture it timely, the next prediction can follow the trend. In addition, the one-time step delay might also be due to that only time index is included in GPR model. It is expected that timely response can be achieved if more information about regeneration is included such as rest time.

The one-step-ahead prediction absolute percentage errors (APE) on batteries No. 5, 6, and 7 are shown in Figures 11A, 11B, and 11C, respectively. It is found that maximum prediction APE of three methods is always observed at regeneration peaks for three batteries and SMK-GPR has larger APE than both SE-MGRP and P-MGPR. It is also seen that for both SE-MGRP and P-MGPR models, the maximum prediction APE on battery No. 5, 6, and 7 are less than 6, 10, and 6%, respectively, and the most of the APE values are less than 1% for three batteries. Moreover, the prediction MAPE and RMSE on three batteries are shown in Figure 12. It is found that SE-MGPR shows a slight better prediction performance than P-MGPR, while SMK-GPR has the largest prediction MAPE and RMSE. The smallest

Table 1. Performance Comparisons of Different Methods for Batteries No. 5, 6, and 7

Battery No.	Error Criteria	Basic GPR[a]	LGPFR[a]	QGPFR[a]	Combination LGPFR[a]	Combination QGPFR[a]	SMK-GPR	P-MGPR	SE-MGPR
5	MAPE(%)	12.10	23.0	1.90	1.60	2.10	1.65	1.55	1.38
	RMSE	13.03	1.71	1.50	1.36	1.80	1.38	1.36	1.20
6	MAPE(%)	27.0	10.30	7.70	10.20	29.0	10.60	2.96	2.93
	RMSE	22.51	6.90	5.12	6.86	20.44	7.08	2.12	2.11
7	MAPE(%)	19.20	1.90	5.40	1.70	2.60	1.91	1.09	1.02
	RMSE	20.70	1.59	5.52	1.73	2.69	1.88	1.14	1.07

[a]Results of these methods are obtained from Ref. 21.

prediction MAPE of SE-MGPR on batteries No. 5, 6, and 7 are 0.60, 0.98, and 0.49%, respectively, and the smallest prediction RMSE of SE-MGPR on batteries No. 5, 6, and 7 are 0.82, 1.33, and 0.72, respectively. The small values of MAPE and RMSE indicate that the multiscale GPR modeling approach can be suitable to perform accurate one-step-ahead SOH prediction and satisfy the engineering requirement.

The computational time for constructing SOH prediction model with six GPR models using both SE-MGPR and P-MGPR is less than 10 s, which is able to meet the online SOH estimation requirement. The computational time of SMK-GPR with exact inference method is approximately four times higher than that of the multiscale GPR model. The possible reason is that the multiscale manner would reduce the data complexity at each scale and the optimization efficiency of GPR model could be greatly improved. For SOC estimation, the actual usable capacity of lithium-ion batteries needs to be estimated at the beginning of each charge/discharge cycle. Since the time of each charge/discharge cycle is generally from several tens of minutes to several hours, such a long time is sufficient to construct the SOH prediction model. Moreover, recent developed online GPR model method can be introduced to further improve the computational efficiency for tackling mass data problem.[32] More importantly, as the model in this study is the original GPR form, there is much room for further improvement, not only in prediction accuracy but also in computational efficiency.

Multi-step-ahead SOH prediction

RUL prognostics require accurate estimation of capacity degradation over a long prediction horizon. To validate the multi-step-ahead SOH prediction ability of the proposed method, we first select the data from cycle 1 to cycle 100 as train set and predict the SOH values from cycle 101 to cycle 168. The prediction MAPE and RMSE of SE-MGPR, P-MGPR, and SMK-GPR on three batteries are then evaluated and compared with the results obtained from Ref. 21. Table 1 shows performance comparisons of different methods for batteries No. 5–7. It can be easy to see that the proposed multiscale GPR modeling method has much better prediction performance than the five published methods and both SE-MGPR and P-MGPR have almost comparable best prediction performance. In comparison with the best results among the five published methods, SMK-GPR is found to be exhibited comparable prediction performance. The smallest prediction MAPE on batteries No. 5, 6, and 7 among the five published models are 1.60, 7.70, and 1.70%, respectively, while the prediction MAPE of SE-MGPR on batteries No. 5, 6, and 7 are 1.38, 2.93, and 1.02%, respectively. Similarly, compared to the five published methods, the prognostic RMSE of

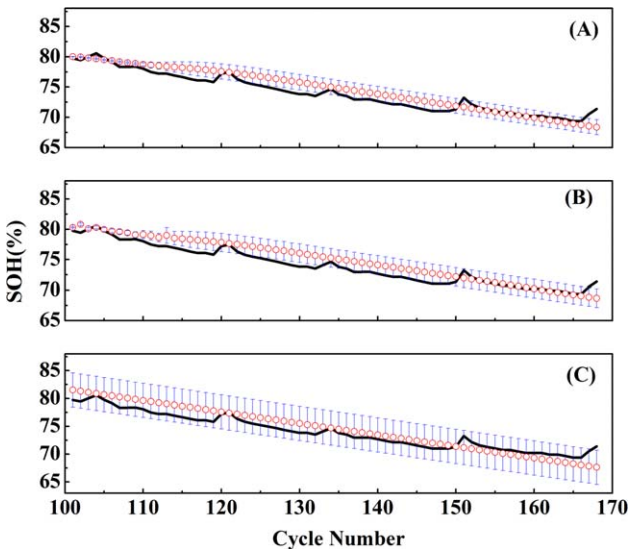

Figure 13. Multi-step-ahead SOH prediction with variance for battery No. 5 using three methods: (A) SE-MGPR; (B) P-MGPR; (C) SMK-GPR.

[Color figure can be viewed in the online issue, which is available at wileyonlinelibrary.com.]

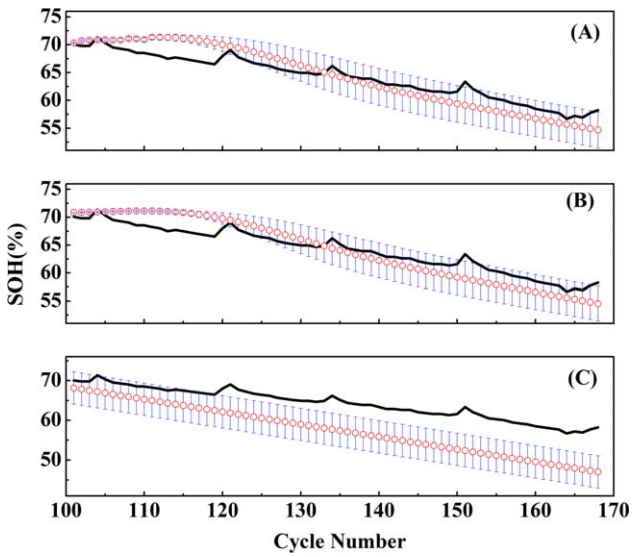

Figure 14. Multi-step-ahead SOH prediction with variance for battery No. 6 using three methods: (A) SE-MGPR; (B) P-MGPR; (C) SMK-GPR.

[Color figure can be viewed in the online issue, which is available at wileyonlinelibrary.com.]

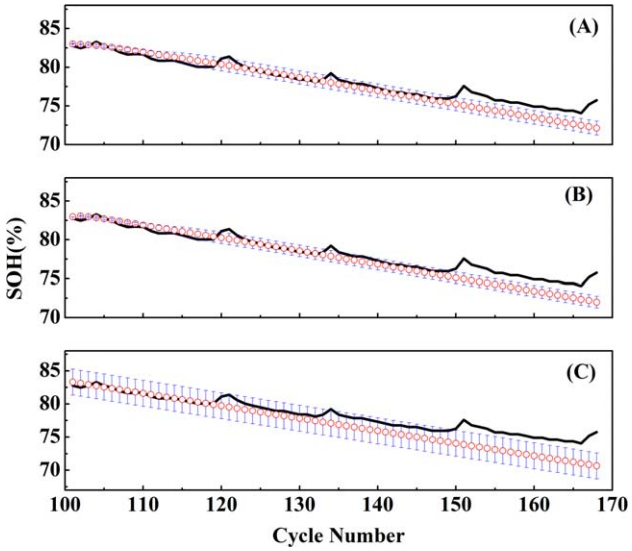

Figure 15. Multi-step-ahead SOH prediction with variance for battery No. 7 using three methods: (A) SE-MGPR; (B) P-MGPR; (C) SMK-GPR.

[Color figure can be viewed in the online issue, which is available at wileyonlinelibrary.com.]

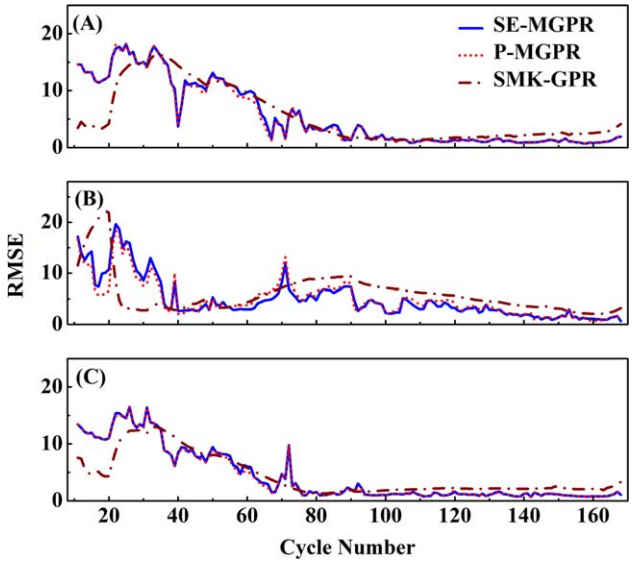

Figure 17. RMSE of multi-step-ahead SOH prediction for three batteries: (A) No. 5; (B) No. 6; (C) No. 7.

[Color figure can be viewed in the online issue, which is available at wileyonlinelibrary.com.]

SE-MGPR on three batteries are also the smallest. It is thus concluded that the multiscale approach could significantly improve the SOH prediction performance. The possible reason is that the extracted approximated signal with a monotonic decrease trend can be easy to be modeled compared to direct modeling of the raw SOH time series corrupted with regeneration and fluctuations. Moreover, the extracted detailed signals seem to be approximately stationary, which would also take advantage of time series prediction method with a lag vector. That further validates our perception that for the long-term SOH prediction, it might be unnecessary to pay more attentions to accurately capture the local regeneration and fluctuations, and the most important task is to correctly track the degradation trend, especially for a very long prediction horizon in RUL prognostics. However, as the operating conditions could significantly affect the degradation rate at different charge/discharge cycles, if the training set does not cover the whole operating range, the data-driven approach might fail to capture the correct trend.

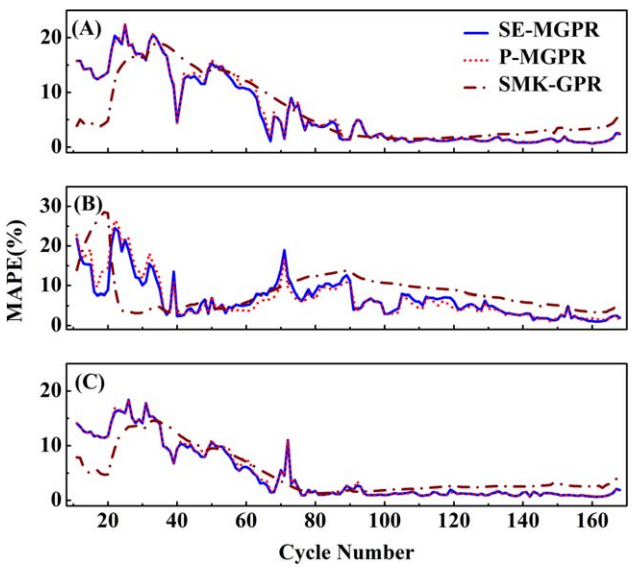

Figure 16. MAPE of multi-step-ahead SOH prediction for three batteries: (A) No. 5; (B) No. 6; (C) No. 7.

[Color figure can be viewed in the online issue, which is available at wileyonlinelibrary.com.]

Figures 13–15 show the multi-step-ahead SOH mean prediction with variance for batteries No. 5–7, respectively. It is observed that the predicted mean SOH of both SE-MGPR and P-MGPR are much closer to the actual SOH curves than that of SMK-GPR. The predicted variances of SE-MGPR and P-MGPR gradually increase with the prognostic process and will keep almost constant after 20, 30, and 20 steps on batteries No. 5, 6, and 7, respectively, whereas for the SMK-GPR, the predicted variances keep constant during the whole prediction horizon. It is also seen that the predicted variances of SMK-GPR are much larger than that of SE-MGPR and P-MGPR for three batteries. As shown in Figures 13A–C, the maximum variances on battery No. 5 are 1.2, 1.5, and 3.1 for SE-MGPR, P-MGPR, and SMK-GPR, respectively. In general, a small prediction variance corresponds to better prediction ability with high confidence. As stated by Liu et al.,[21] both mean and variance should be simultaneously evaluated for making the prognostics better. Conversely, it is found that the long-term predictions of three methods almost become linear after a while. One possible reason could be that the effect of covariance function reduces at points far away from the training set and predictions approach the mean function for GPR.

Moreover, the effect of the size of training set, varying from 10 to 167, on the multi-step-ahead SOH prediction performance, is thoroughly investigated. The number of training samples increases with the increasing of the charge/discharge cycles. Figures 16 and 17 plot the MAPE and RMSE of multi-step-ahead SOH prediction against cycle, respectively. As shown in Figure 16, the MAPE on three batteries

gradually decreases with the increasing of the charge/discharge cycles. The RMSE from Figure 17 also shows the similar results as Figure 16. The main reason is that the error of multi-step-ahead time series prediction often accumulates step-by-step and the available of more training samples would be helpful to decrease the prediction error. Both SE-MGPR and P-MGPR show comparable prediction performance on three batteries. It is also found that the MAPE of SMK-GPR is larger than that of SE-MGPR and P-MGPR at higher cycle region. It further validates the effectiveness of the multiscale modeling approach. Moreover, it is observed that after gathering about 80 SOH samples, both MAPE and RMSE of SE-MGPR and P-MGPR on three batteries are shown to keep almost constant with little fluctuations. It needs to be mentioned that the main aim of performing multi-step-ahead SOH prediction is to carry out RUL prognostics for safe and reliable operation of lithium-ion batteries, and in general the prognostic performance of RUL for batteries at the early period is not so important for most of the circumstance, except for the extreme conditions that the monitored batteries are damaged at early period. Based on the given datasets, lithium-ion batteries with 80 charge/discharge cycles are only at their intermediate stage of the whole life. It is thus concluded that the proposed multiscale method is able to provide an accurate long-term SOH prediction for assisting in RUL prognostics. Moreover, note that the recent developed novel strategies[23,24] such as DirRec, MIMO, and DIRMO can be worth investigating under the proposed multiscale modeling framework to further improve the long-term prediction performance.

Conclusions

A multiscale GPR model is proposed to SOH prediction of lithium-ion batteries. Wavelet analysis method is applied to decouple the global degradation, local regeneration, and fluctuations in SOH time series. Then, GPR with the inclusion of time index is utilized to fit the extracted global degradation trend, and GPR with the input of lag vector is designed to recursively predict local regeneration and fluctuations. Three datasets of lithium-ion batteries obtained from the data repository of the NASA Ames PCoE are used to illustrate the effectiveness of the proposed method. The main findings of the present study can be summarized as follows:

1. Based on the wavelet decomposition of SOH time series, a smooth monotonic degradation trend is extracted; the level 1–3 and level 4–5 detailed signals are related to capacity regeneration and local performance fluctuations, respectively. Energy distribution analysis shows the energy percentage of the level-1 detailed signal might be closely related to capacity degradation rate for different batteries. The multiscale characteristics of SOH time series are obviously observed and multiscale decomposition of SOH time series could be helpful to obtain more useful information, reduce the modeling complexity, and improve the prediction performance.

2. Both one-step-ahead and multi-step-ahead SOH predictions illustrate the effectiveness of the proposed multiscale GPR modeling method. For the one-step-ahead prediction, the predicted SOH is very close to the actual SOH, and the smallest MAPE on batteries No. 5, 6, and 7 are 0.60, 0.98, and 0.49%, respectively. For the multi-step-ahead prediction, the proposed method outperforms the combination GPR model and SMK-GPR without multiscale decomposition in terms of the prediction MAPE and RMSE, and the performance of long-term SOH prediction will increase with the increase of the training samples. Moreover, the computational time is less than 10 s, which is much lower than one charge/discharge cycle. The results, therefore, indicate that the multiscale GPR modeling approach provides a unified framework for accurate and rapid SOH prediction, which is helpful to SOC estimation and RUL prognostics. More importantly, it should be noted that the proposed method could be extended to other health management systems with the multiscale characteristics.

Acknowledgments

This work was supported by the National Basic Research Program of China (2014CB239703) and the National Natural Science Foundation of China (21006084, 21336003) and the Science and Technology Commission of Shanghai Municipality (14DZ2250800). The authors would also like to thank anonymous reviewers for their valuable comments.

Literature Cited

1. Zhang J, Lee J. A review on prognostics and health monitoring of Li-ion battery. *J Power Sources*. 2011;196:6007–6014.
2. Saha B, Goebel K, Poll S, Christophersen J. Prognostics methods for battery health monitoring using a Bayesian framework. *IEEE Trans Instrum Meas*. 2009;58:291–296.
3. Olivares BE, Muñoz MAC, Orchard ME, Silva JF. Particle-filtering-based prognosis framework for energy storage devices with a statistical characterization of state-of-health regeneration phenomena. *IEEE Trans Instrum Meas*. 2013;62:364–376.
4. Santhanagopalan S, Zhang Q, Kumaresan K, White RE. Parameter estimation and life modeling of lithium-ion cells. *J Electrochem Soc*. 2008;155:A345–A353.
5. Ploehn HJ, Ramadass P, White RE. Solvent diffusion model for aging of lithium-ion battery cells. *J Electrochem Soc*. 2004;151:A456–A462.
6. Christensen J, Newman J. Cyclable lithium and capacity loss in Li-ion cells. *J Electrochem Soc*. 2005;152:A818–A829.
7. Saha B, Goebel K. Modeling Li-ion battery capacity depletion in a particle filtering framework. In: *Annual Conference of the Prognostics and Health Management Society*. San Diego, CA: PHM Society, 2009:1–10.
8. Bhangu BS, Bentley P, Stone DA, Bingham CM. Nonlinear observers for predicting state-of-charge and state-of-health of lead-acid batteries for hybrid-electric vehicles. *IEEE Trans Veh Technol*. 2005;54:783–794.
9. Dai H, Wei X, Sun Z. A new SOH prediction concept for the power lithium-ion battery used on HEVs. In: *Vehicle Power and Propulsion Conference*. Dearborn, MI: IEEE Press, 2009:1649–1653.
10. Saha B, Goebel K. Uncertainty management for diagnostics and prognostics of batteries using Bayesian techniques. In: *2008 IEEE Aerospace Conference*. Big Sky, MT: IEEE Press, 2008:1–8.
11. Goebel K, Saha B, Saxena A, Celaya JR, Christophersen JP. Prognostics in battery health management. *IEEE Instrum Meas Mag*. 2008;11:33–40.
12. He W, Williard N, Osterman M, Pecht M. Prognostics of lithium-ion batteries based on Dempster–Shafer theory and the Bayesian Monte Carlo method. *J Power Sources*. 2011;196:10314–10321.
13. Orchard M, Tang L, Saha B, Goebel K, Vachtsevanos G. Risk sensitive particle-filtering-based prognosis framework for estimation of remaining useful life in energy storage devices. *Stud Inf Control*. 2010;19:209–218.
14. Hu C, Jain G, Tamirisa P, Gorka T. Method for estimating capacity and predicting remaining useful life of lithium-ion battery. *Appl Energy*. 2014;126:182–189.
15. Qian K, Zhou C, Yuan Y, Allan M. Temperature effect on electric vehicle battery cycle life in vehicle-to-grid applications. In: *2010 China International Conference on Electricity Distribution*. Nanjing, China: IEEE Press, 2010:1–6.
16. Salkind AJ, Fennie C, Singh P, Atwater T, Reisner DE. Determination of state-of-charge and state-of-health of batteries by fuzzy logic methodology. *J Power Sources*. 1999;80:293–300.

17. Pattipati B, Pattipati K, Christopherson JP, Namburu SM, Prokhorov DV, Qiao L. Automotive battery management systems. In: IEEE Autotestcon. Salt Lake City, UT: IEEE Press, 2008:581–586.
18. Chen H, Li X. Distributed active learning with application to battery health management. In: *Proceedings of the 14th International Conference on Information Fusion*. Chicago, IL: IEEE Press, 2011:1–7.
19. Wang D, Miao Q, Pecht M. Prognostics of lithium-ion batteries based on relevance vectors and a conditional three-parameter capacity degradation model. *J Power Sources*. 2103;239:253–264.
20. Rasmussen CE, Williams CKI. *Gaussian Processes for Machine Learning*. Cambridge, MA: MIT Press, 2006.
21. Liu D, Pang J, Zhou J, Peng Y, Pecht M. Prognostics for state of health estimation of lithium-ion batteries based on combination Gaussian process functional regression. *Microelectron Reliab*. 2013;53:832–839.
22. Misiti M, Misiti Y, Oppenheim G, Poggi J. Wavelets and Their Applications. London: ISTE Publishing Company, 2007.
23. Taieb SB, Bontempi G, Atiya AF, Sorjamaa A. A review and comparison of strategies for multi-step ahead time series forecasting based on the NN5 forecasting competition. *Expert Syst Appl*. 2012; 39:7607–7083.
24. Sorjamaa A, Hao J, Reyhani N, Ji Y, Lendasse A. Methodology for long-term prediction of time series. *Neurocomputing*. 2007;70:2861–2869.
25. Wu Z, Huang NE, Long SR, Peng CK. On the trend, detrending, and variability of nonlinear and nonstationary time series. *PNAS*. 2007;104:14889–14894.
26. Williams CKI. Prediction with Gaussian processes: from linear regression to linear prediction and beyond. In: Jordan MI, editor. Learning and Inference in Graphical Models. the Netherlands: Kluwer Academic Press, 1998:599–621.
27. Brahim-Belhouari S, Bermak A. Gaussian process for nonstationary time series prediction. *Comput Stat Data Anal*. 2004;47:705–712.
28. Kocijan J, Girard A, Banko B, Smith MR. Dynamic systems identification with Gaussian processes. *Math Comput Model Dyn Syst*. 2005;11:411–424.
29. Hachino T, Kadirkamanathan V. Time series forecasting using multiple Gaussian process prior model. In: *Proceedings of the 2007 IEEE Symposium on Computational Intelligence and Data Mining*. Honolulu, Hawaii: IEEE Press, 2007:604–609.
30. Wilson AG, Adams RP. Gaussian process kernels for pattern discovery and extrapolation. In: *Proceedings of the 30th International Conference on Machine Learning*. Atlanta, GA: JMLR W&CP, 2013:1067–1075.
31. Saha B, Goebel K. *Battery Data Set, NASA Ames Prognostics Data Repository*. Moffett Field, CA: NASA Ames, 2015, Available at http://ti.arc.nasa.gov/tech/dash/pcoe/prognostic-data-repository.
32. Ranganathan A, Yang MH, Ho J. Online sparse Gaussian process regression and its application. *IEEE Trans Image Process*. 2011;20: 391–404.

Manuscript received Oct. 31, 2014, and revision received Jan. 29, 2015.